Direct Torque and Indirect Flux Control of Brushless DC Motor

Salih Baris Ozturk, *Member, IEEE*, and Hamid A. Toliyat, *Fellow, IEEE*

***Abstract*—In this paper, the position-sensorless direct torque and indirect flux control of brushless dc (BLDC) motor with nonsinusoidal back electromotive force (EMF) has been extensively investigated. In the literature, several methods have been proposed for BLDC motor drives to obtain optimum current and torque control with minimum torque pulsations. Most methods are complicated and do not consider the stator flux linkage control, therefore, possible high-speed operations are not feasible. In this study, a novel and simple approach to achieve a low-frequency torque ripple-free direct torque control (DTC) with maximum efficiency based on *dq* reference frame is presented. The proposed sensorless method closely resembles the conventional DTC scheme used for sinusoidal ac motors such that it controls the torque directly and stator flux amplitude indirectly using *d*-axis current. This method does not require pulsewidth modulation and proportional plus integral regulators and also permits the regulation of varying signals. Furthermore, to eliminate the low-frequency torque oscillations, two actual and easily available line-to-line back EMF constants (k_{ba} and k_{ca}) according to electrical rotor position are obtained offline and converted to the *dq* frame equivalents using the new line-to-line park transformation. Then, they are set up in the look-up table for torque estimation. The validity and practical applications of the proposed sensorless three-phase conduction DTC of BLDC motor drive scheme are verified through simulations and experimental results.**

***Index Terms*—Brushless dc (BLDC) motor, direct torque control (DTC), fast torque response, low-frequency torque ripples, nonsinusoidal back electromotive force (EMF), position-sensorless control, stator flux control, torque pulsation.**

I. Introduction

THE permanent-magnet synchronous motor (PMSM) and brushless dc (BLDC) motor drives are used extensively in several high-performance applications, ranging from servos to traction drives, due to several distinct advantages such as high power density, high efficiency, large torque to inertia ratio, and simplicity in their control [1]–[3].

In many applications, obtaining a low-frequency ripple-free torque and instantaneous torque and even flux control are of primary concern for BLDC motors with nonsinusoidal back electromotive force (EMF). A great deal of study has been devoted to the current and torque control methods employed for BLDC motor drives. One of the most popular approaches is a generalized harmonic injection approach by numerical optimization solutions to find out optimal current waveforms based on back EMF harmonics to minimize mutual and cogging torque [4]–[15]. Those approaches limit Fourier coefficients up to an arbitrary high harmonic order due to calculation complexity [16]. Moreover, obtaining those harmonics and driving the motor by pulsewidth modulation (PWM) method complicates the real-time implementation. Optimal current references are not constant and require very fast controllers especially when the motor operates at high speed. Moreover, the bandwidth of the classical proportional plus integral (PI) controllers does not allow tracking all of the reference current harmonics. Since the torque is not controlled directly, fast torque response cannot be achieved. Also, the rotor speed is measured by an expensive position sensor.

Ha and Kang [17] completely characterized, in an explicit form, the class of feedback controllers that produce ripple free torque in brushless motors. A free function can be used to achieve other control objectives such as minimization of power dissipation, but phase current saturation was not considered [18]. Also, flux-weakening performance and experimental results are not provided. Aghili *et al.* [18] presents the optimal torque control of general multiphase brushless motors based on quadratic programming equality and inequality constraints via Kuhn–Tucker theorem. Copper losses and torque ripples are minimized and the torque capability is maximized under current limitation. However, expensive experimental setup is required which includes high resolution encoder, torque transducer, and hydraulic dynamometer. Moreover, the operation of the proposed method in the flux-weakening region is not demonstrated.

In [19], electromagnetic torque is calculated from the product of the instantaneous back EMF and current both in two-phase and in the commutation period. Then, the prestored phase back EMF values are obtained using midprecision position sensor. As a result, torque pulsations due to the commutation are reduced. However, phase resistance is neglected and the torque estimation depends on parameters such as dc-link voltage and phase inductance. Moreover, instead of a simple voltage selection look-up table technique more sophisticated PWM method is used to drive the BLDC motor. Also, two phase conduction method instead of a three-phase one is used which is problematic in the high speed applications.

In [20], the disadvantages observed in [13]–[15] are claimed to be improved by proposing a new instantaneous torque control. It is based on the model reference adaptive system (MRAS)

Manuscript received May 30, 2009; revised September 11, 2009 and January 2, 2010; accepted February 6, 2010. Date of publication March 25, 2010; date of current version January 19, 2011. Recommended by Technical Editor M.-Y. Chow.

S. B. Ozturk is with the Faculty of Engineering and Architecture, Okan University, Akfirat Campus, Tuzla/Istanbul 34959, Turkey (e-mail: salihbaris@gmail.com).

H. A. Toliyat is with the Department of Electrical and Computer Engineering, Texas A&M University, College Station, TX 77843-3128 USA (e-mail: toliyat@ece.tamu.edu).

Color versions of one or more of the figures in this paper are available online at http://ieeexplore.ieee.org.

Digital Object Identifier 10.1109/TMECH.2010.2043742

technique and the torque is calculated by using the estimated flux and measured current. Then, the torque is instantaneously controlled by the torque controller using the integral variable structure control (IVSC) and the space-vector PWM (SVPWM). However, this technique increases the complexity of the control system.

The optimum current excitation methods, considering the unbalanced three-phase stator windings as well as nonidentical and half-wave asymmetric back EMF waveforms in BLDC motor, are reported in [16] and [21]. These methods avoid the complicated harmonic coefficient calculation based on the optimization approach. Hysteresis current controllers with PWM generation, which increases the complexity of the drive, are used to drive the BLDC motor. In [21], several transformations are required in order to get the *abc* frame optimum reference current waveforms. These transformations complicate the control algorithm and the scheme could not directly control the torque, therefore, fast torque response cannot be achieved. In both methods, three offline measured back EMF waveforms are needed for the torque estimation. Moreover, stator flux is not controlled, therefore, high speed applications cannot easily be performed.

In [22] and [23], the method of multiple reference frames is employed in the development of a state variable model for BLDC drives with nonsinusoidal back EMF waveforms. This method involves tedious algorithms, which increase the complexity of the control system. Moreover, in [22], to determine the right d-axis current in flux-weakening region the high order d-axis harmonic current values are required which are quite difficult to obtain. Also, the back EMF is assumed to be ideal trapezoidal and its harmonics higher than seventh order are neglected which results in a reduction of the accuracy in the overall system.

Direct torque control (DTC) scheme was first proposed by Takahashi and Noguchi [24] and Depenbrock [25] for induction motor drives in the mid-1980s. More than a decade later, in the late 1990s, DTC techniques for both interior and surface-mounted PMSM were analyzed [26]. More recently, application of conventional DTC scheme is extended to BLDC motor drives [27], [28]. In [27] and [28], the voltage space vectors in a two-phase conduction mode are defined and a stationary reference frame electromagnetic torque equation is derived for surface-mounted permanent magnet synchronous machines with nonsinusoidal back EMF (BLDC, etc.). It is shown in [28] that only electromagnetic torque in the DTC of BLDC motor drive under two-phase conduction mode can be controlled. Flux control is not trivial due to the sharp changes whose amplitudes are unpredictable depending on several factors such as load torque, dc-link voltage, winding inductance, etc.

This study presents a novel and simple position-sensorless direct torque and indirect flux control of BLDC motor that is similar to the conventional DTC scheme used for sinusoidal ac motors where both torque and flux are controlled, simultaneously. This method provides advantages of the classical DTC such as fast torque response compared to vector control, simplicity (no PWM strategies, PI controllers, and inverse Park and inverse Clarke transformations), and a position-sensorless drive. As opposed to the prior two-phase conduction direct torque control methods used for BLDC motor [27], [28], the proposed DTC technique provides position-sensorless drive that is quite similar to the one used in conventional DTC scheme and also controls the stator flux indirectly using d-axis current. Therefore, flux-weakening operation is possible. Coordinate transformations are done by the new line-to-line Park transformation that forms a 2×2 matrix instead of the conventional 2×3 matrix. Therefore, rather than three line-to-neutral back EMF waveforms, which are not directly available in the motor easily accessible two line-to-line back EMF constants ($k_{ba}(\theta_{re})$ and $k_{ca}(\theta_{re})$) are obtained offline and converted to the *dq* frame equivalents ($k_d(\theta_{re})$ and $k_q(\theta_{re})$). Then, they are stored in a look-up table for the torque estimation. The electrical rotor position is estimated using winding inductance and stationary reference frame stator flux linkages and currents. Since the hysteresis controllers used in the proposed DTC scheme are not fast controllers like PI, they can easily regulate not only constant, but also the varying references (torque and flux). Simulation and experimental results are presented to illustrate the validity and effectiveness of the sensorless three-phase conduction DTC of a BLDC motor drive.

II. Proposed Line-to-Line Park and Clarke Transformations in 2×2 Matrix Form

Since the balanced systems in *dq*-axes reference frame do not require a zero sequence term, first line-to-line Clarke transformation from the balanced three-phase quantities is derived and, then the line-to-line Park transformation forming a 2×2 matrix instead of a 2×3 matrix for three-phase systems can be obtained in the following.

Using some algebraic manipulations, the original Clarke transformation forming a 2×3 matrix excluding the zero-sequence term can be simplified to a 2×2 matrix as follows:

$$[T_{LL}] = \begin{bmatrix} -\frac{1}{3} & -\frac{1}{3} \\ \frac{\sqrt{3}}{3} & -\frac{\sqrt{3}}{3} \end{bmatrix} \tag{1}$$

which requires only two input variables X_{ba} and X_{ca} where $X_{ba} = X_b - X_a$ and $X_{ca} = X_c - X_a$. X represents machine variables such as currents, voltages, flux linkages, back EMFs, etc.

To obtain the line-to-line Park transformation forming a 2×2 matrix, the inverse of the original Clarke transformation matrix $[T_{\alpha\beta}]$ is required. Since the zero-sequence term is removed, $[T_{\alpha\beta}]$ matrix is not square anymore, but it is still singular and therefore, pseudoinverse can be found in the following:

$$[T_{\alpha\beta}]^{+} = [T_{\alpha\beta}]^{T}([T_{\alpha\beta}][T_{\alpha\beta}]^{T})^{-1} \tag{2}$$

where $[T_{\alpha\beta}]^{+}$ and $[T_{\alpha\beta}]^{T}$ are the pseudoinverse and transpose of the original Clarke transformation matrix $[T_{\alpha\beta}]$, respectively.

Here *abc* to *ba–ca* transformation can be represented as follows:

$$[T_{\alpha\beta}]^{+}[T_{\alpha\beta}] \begin{bmatrix} X_a \\ X_b \\ X_c \end{bmatrix} = [T_{\alpha\beta}]^{+}[T_{LL}] \begin{bmatrix} X_{ba} \\ X_{ca} \end{bmatrix}. \tag{3}$$

After (3) is expanded and multiplied by the original 2×3 Park transformation matrix in both sides, algebraic manipulations lead to simplifications using some trigonometric equivalence. Therefore, the following 2×2 line-to-line Park transformation matrix form is obtained:

$$\begin{bmatrix} X_d \\ X_q \end{bmatrix} = \frac{2}{3} \begin{bmatrix} \sin\left(\theta - \frac{\pi}{6}\right) & -\sin\left(\theta + \frac{\pi}{6}\right) \\ -\cos\left(\theta - \frac{\pi}{6}\right) & \cos\left(\theta + \frac{\pi}{6}\right) \end{bmatrix} \begin{bmatrix} X_{ba} \\ X_{ca} \end{bmatrix}. \tag{4}$$

III. Proposed Sensorless DTC of BLDC Motor Drive Using Three-Phase Conduction

A. Principles of the Proposed Method

In this study, indirect torque control method of BLDC motor explained in [29] is extended to a direct torque and indirect flux control technique, which is suitable for sensorless and flux-weakening operations. The proposed method transforms *abc* frame quantities to *dq* frame ones using the new 2×2 line-to-line Park transformation matrix. Rather than three measured phase back EMFs, which are used in [29], in the proposed balanced system only two electrical rotor position dependant back EMF constants ($k_d(\theta_{re})$ and $k_q(\theta_{re})$) are required in the torque estimation algorithm. Since the numbers of input variables (current and back EMF) are reduced from three to two, much simpler Park transformation can be used as given in (4). Therefore, the amount of multiplications and sine/cosine functions are minimized.

Unlike previous two-phase conduction DTC of BLDC motor drive techniques, which are proposed in [27] and [28], this method uses DTC technique with three-phase conduction, therefore, flux-weakening operation as well as a much simpler sensorless technique can easily be achieved. Compared with the two-phase conduction DTC scheme, this DTC method differs by its torque estimation and voltage vector selection table which is similar to the one used for DTC of PMSM drives explained in [30]. Although, stator flux estimation algorithm in both methods (two-phase and three-phase conduction) is the same due to the similar machine model in which the back EMF shape separates the two from each other, in two-phase conduction scheme the stator flux amplitude is uncontrollable. Since the proposed technique adopts three-phase conduction, there is a possibility to control the stator flux amplitude without commutation issue, therefore, flux-weakening and sensorless operations that involve back EMF estimation can easily be performed. Moreover, this DTC method controls the voltage vectors directly from a simple look-up table depending on the outcome of hysteresis torque and indirect flux controllers, thus the overall control is much simpler and faster torque response can be achieved compared to the conventional PWM control techniques.

For machines with surface-mount magnet rotor (BLDC) stator flux linkages in rotor *dq* reference frame can be written as

$$\varphi_{qs}^r = L_s i_{ds}^r + \varphi_r' \sum_{n=1}^{\infty} (K_{6n-1} + K_{6n+1}) \sin(6n\theta_r) \tag{5}$$

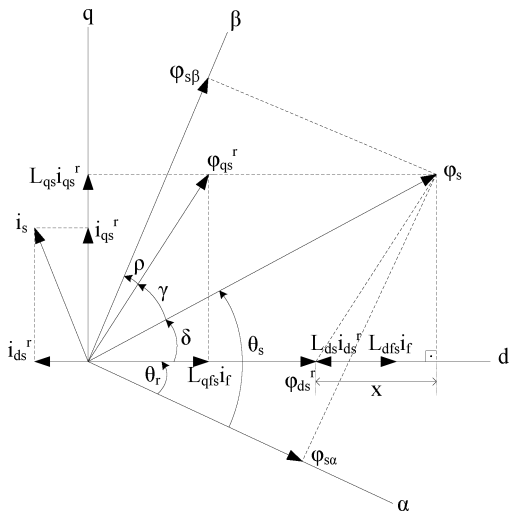

Fig. 1. Rotor and stator flux linkages of a BLDC motor in the stationary $\alpha\beta$-plane and synchronous *dq*-plane [31].

$$\varphi_{ds}^r = L_s i_{qs}^r + \varphi_r' \sum_{n=1}^{\infty} (K_{6n-1} - K_{6n+1}) \cos(6n\theta_r) + \varphi_r' \tag{6}$$

where φ_r' is the peak value of the fundamental rotor magnetic flux linkage of the BLDC motor, the coefficients K_{6n-1} and K_{6n+1} represent the odd harmonics of the phase back EMF other than the third and its multiples. K_{6n-1} equals $[\sin(6n-1)\sigma]/[(6n-1)^3 \sin\sigma]$, and K_{6n+1} can be depicted as $[\sin(6n+1)\sigma]/[(6n+1)^3 \sin\sigma]$. σ is the angle between zero-crossing and phase back EMF, where it becomes flat at the top. Fundamental peak value of the rotor magnet flux linkage φ_r' equals $(4k_e/\sigma\pi)\sin\sigma$, where k_e is the line-to-neutral back EMF constant.

Equations (5) and (6) are very close approximations of stator flux linkages in *dq* reference frame for the PMSM with non-sinusoidal back EMF. It can be seen that they are not constant as in pure sinusoidal ac machines. Inductances and stator flux linkages vary by the six times of the fundamental frequency. One of the reasons to derive the equivalent inductance and then the *dq* frame stator flux linkages in BLDC motor is that it can be easily observable which parameters affect the amplitude of the stator flux linkages. Stator flux linkage amplitude $|\varphi_s| = \sqrt{(\varphi_{ds}^{r2} + \varphi_{qs}^{r2})}$ can be changed by varying the *d*-axis current i_{ds}^r in (11) assuming the torque is constant and it is proportional to i_{qs}^r; therefore, an indirect flux control can be achieved in the proposed DTC of BLDC motor drive.

Although i_{qs}^r is assumed constant meaning that it has an offset to generate an average torque, to obtain a smooth electromagnetic torque it varies by six times the fundamental frequency because flux harmonics given in (5) and (6) generate torque pulsations on the order of six and multiples of six. The *d*-axis current reference is selected zero when the motor operates in the constant torque region (below flux-weakening region). The phasor diagram for stator flux linkage vectors in BLDC motor can be drawn in the rotor *dq* and stationary ($\alpha\beta$) reference frames as

shown in Fig. 1, where $L_{ds} = L_{qs} = L_s$ and $L_{dqs} = L_{qds} = 0$. L_{dqs} and L_{qds} are the mutual inductances between *d*- and *q*-axis. L_{dsf} and L_{qsf} are the mutual inductances between *dq*-axes and permanent magnet (PM), respectively, and i_f is the equivalent current generated by PM. In Fig. 1, unlike PMSM with sinusoidal back EMF synchronous reference frame flux linkages φ_{qs}^r and φ_{ds}^r vary with time, therefore, stator flux amplitude $|\varphi_s|$ is not constant anymore. γ, ρ, and δ in Fig. 1 can be obtained, respectively, as

$$\gamma = \sin^{-1}\left(\frac{L_{qs} i_{qs}^r}{\varphi_{qs}^r}\right) + \cos^{-1}\left(\frac{L_{qs} i_{qs}^r}{\varphi_s}\right) - \frac{\pi}{2} \tag{7}$$

$$\rho = -\left(\theta_s + \gamma - \frac{\pi}{2}\right) \tag{8}$$

and

$$\delta = \frac{\pi}{2} - \cos^{-1}\left(\frac{L_{qs} i_{qs}^r}{\varphi_s}\right). \tag{9}$$

Moreover, x in Fig. 1 can be expressed as

$$x = \varphi_{qs}^r \cos\left[\sin^{-1}\left(\frac{L_{qs} i_{qs}^r}{\varphi_s}\right)\right]. \tag{10}$$

B. Electromagnetic Torque Estimation in dq Reference Frame

Because of the rotor position dependant terms in the *dq* frame stator flux linkages in (5) and (6) and inductances, conventional torque estimation in stator reference frame used for DTC of sinusoidal ac motors is no longer valid for BLDC motor, therefore, a new torque estimation algorithm is derived in *dq* frame consisting of actual *dq*-axes back EMF constants and currents. Instead of the actual back EMF waveforms, Fourier approximation of the back EMFs could have been adopted in torque estimation, but the results would not truly represent the reality and more complex computations are required.

The torque estimation is the key factor in the proposed DTC scheme. First, two line-to-line back EMF waveforms $e_{ba}(\theta_{re})$ and $e_{ca}(\theta_{re})$ are obtained offline and converted to the *ba–ca* frame back EMF constants $k_{ba}(\theta_{re})$ and $k_{ca}(\theta_{re})$. The line-to-line Park transformation matrix in (4) is used to obtain the *dq* reference frame back EMF constants $k_d(\theta_{re})$ and $k_q(\theta_{re})$, where θ_{re} is the electrical rotor angular position. Then, they are stored in a look-up table for electromagnetic torque estimation.

The electromagnetic torque $T_{\rm em}$ estimation algorithm can be derived for a balanced system in *dq* reference frame by equating the electrical power absorbed by the motor to the mechanical power produced ($P_i = P_m = T_{\rm em}\omega_m$) as follows:

$$\begin{aligned} T_{\rm em} &= \frac{3P}{4\omega_{re}}(e_q(\theta_{re}) i_{qs}^r + e_d(\theta_{re}) i_{ds}^r) \\ &= \frac{3P}{4}(k_q(\theta_{re}) i_{qs}^r + k_d(\theta_{re}) i_{ds}^r) \end{aligned} \tag{11}$$

where P is the number of poles, ω_{re} is the electrical rotor speed, $e_q(\theta_e)$ and $e_d(\theta_e)$, i_{qs}^r and i_{ds}^r, $k_q(\theta_e)$, and $k_d(\theta_e)$ are the *dq*-axes back EMFs, currents, and back EMF constants according to the electrical rotor position, respectively. As it can be noticed that the right-hand side equation in (11) eliminates the speed term in the denominator which causes problem at zero and near zero speeds.

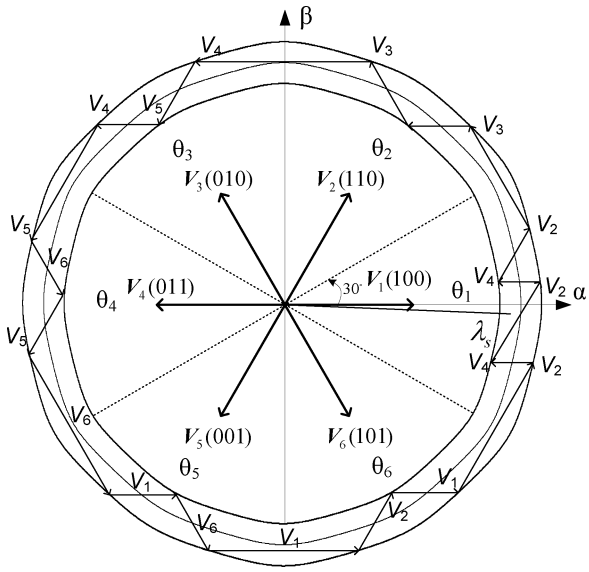

Fig. 2. Dodecagon trajectory of stator flux linkage in the stationary $\alpha\beta$-plane.

C. Control of Stator Flux Linkage Amplitude

The stator flux linkage equations of a BLDC motor can easily be represented in the stationary reference frame similar to PMSM. During the sampling interval time, one out of the six voltage vectors is applied, and each voltage vector applied during the predefined sampling interval is constant, then the stator flux estimation for BLDC motor can be written as

$$\begin{aligned} \varphi_{s\alpha} &= V_{s\alpha} t - R_s \int i_{s\alpha} dt + \varphi_{s\alpha}(0) \\ \varphi_{s\beta} &= V_{s\beta} t - R_s \int i_{s\beta} dt + \varphi_{s\beta}(0) \end{aligned} \tag{12}$$

where $\varphi_{s\alpha}(0)$ and $\varphi_{s\beta}(0)$ are the initial stator flux linkages at the instant of switching. If the line-to-line back EMF constant k_{LL} is roughly known, and let say the rotor is brought to zero position (phase a), initial stator flux linkages at start-up can be obtained by integrating the back EMF in which the ideal trapezoidal is assumed. Therefore, approximate initial starting flux values at zero position can be obtained as $\varphi_{s\alpha}(0) = 2k_{LL}\pi/(3\sqrt{3})$ and $\varphi_{s\beta}(0) = 0$.

Since BLDC motor does not have sinusoidal back EMF, the stator flux trajectory is not pure circle as in PMSM. It is more like a decagonal shape as shown in Fig. 2. Thus, direct stator flux amplitude control in a BLDC motor is not trivial as in PMSM such that rotor position varying flux command should be considered. However, this is a complicated way to control the stator flux linkage amplitude. Therefore, in this study, instead of $|\varphi_s|$ itself its amplitude is indirectly controlled by *d*-axis current. In the constant torque region, i_{ds}^r is controlled as zero, and in the flux-weakening region it is decreased for a certain amount depending on the operational speed to achieve maximum torque. As a result, in this study, stator flux linkage amplitude is

TABLE I
SWITCHING TABLE FOR DTC OF BLDC MOTOR USING THREE-PHASE CONDUCTION

φ	τ	θ					
		θ(1)	θ(2)	θ(3)	θ(4)	θ(5)	θ(6)
φ = 1	τ = 1	V_2(110)	V_3(010)	V_4(011)	V_5(001)	V_6(101)	V_1(100)
	τ = -1	V_6(101)	V_1(100)	V_2(110)	V_3(010)	V_4(011)	V_5(001)
φ = -1	τ = 1	V_3(010)	V_4(011)	V_5(001)	V_6(101)	V_1(100)	V_2(110)
	τ = -1	V_5(001)	V_6(101)	V_1(100)	V_2(110)	V_3(010)	V_4(011)

indirectly kept at its optimum level, while the motor speed is less than the base speed.

The switching table for controlling both the amplitude and rotating direction of the stator flux linkage is given in Table I. where the output of the torque hysteresis comparator is denoted as τ, the output of the flux hysteresis comparator as φ, and the flux linkage sector is denoted as θ. The torque hysteresis comparator τ is a two valued comparator; $\tau = -1$ means that the actual value of the torque is above the reference and out of the hysteresis limit and $\tau = 1$ means that the actual value is below the reference and out of the hysteresis limit. The same logic applies to the flux related part of the control (d-axis current). The one out of six voltage space vectors is selected using look-up table in every sampling time to provide fast rotation of stator flux linkage vector. Therefore, fast torque and flux responses are obtained in a predefined hysteresis bandwidth, which limits the flux amplitude.

D. Estimation of Electrical Rotor Position

Electrical rotor position θ_{re}, which is required in the line-to-line Park transformation and torque estimation algorithm can be found by

$$\theta_{re} = \tan^{-1}\left(\frac{\varphi_{s\beta} - L_s i_{s\beta}}{\varphi_{s\alpha} - L_s i_{s\alpha}}\right). \tag{13}$$

To solve the common problems for integrators, a special integration algorithm for estimating the stator flux linkage proposed in [32] is used in this study. Although the method in [32] is designed for sinewave systems, the algorithm is still applicable to a BLDC motor with varying stator flux linkage amplitude as shown in Fig. 2. The second algorithm in [32], which is the modified integrator with an amplitude limiter is used for the stator flux linkage estimation. The maximum amplitude of the stator flux linkage reference approximated as $2k_{LL}\pi/(3\sqrt{3})$ is set for the limiter when the motor speed is less than the base speed. If the motor operates in the flux-weakening region, the limiter value should be selected properly, but this is not in the scope of this paper.

IV. SIMULATION AND EXPERIMENTAL RESULTS

The drive system shown in Fig. 3 has been simulated in order to demonstrate the validity of the proposed three-phase conduction DTC of a BLDC motor drive scheme using line-to-line machine model. The sampling interval is 15 μs. The magnitudes of the torque and flux hysteresis bands are 0.001 N·m and 0.001 Wb, respectively. The dc-link voltage $V_{\rm dc}$ equals $40\sqrt{2}$ V. Appendix I shows the specifications and parameters of the BLDC motor.

In Fig. 4, the possibility of the flux-weakening region operation is simulated when i_{ds}^{r*} is changed from 0 to -5 A. As it can be seen in Fig. 4 that the shape of stator flux linkage trajectory is kept same, however, its amplitude is smaller compared to the initial case, which means that the flux in the machine is weakened to obtain maximum possible torque above the base speed. It is concluded that in the proposed control scheme flux-weakening operation is viable by properly selecting the d-axis current reference as in PMSM drives. As a result, there is no need to use position-varying stator flux linkage amplitude $|\varphi_s(\theta_{re})|^*$ as a reference, which is complicated to obtain especially in the flux-weakening region. Proper selection of the d-axis current reference respective of speed for flux-weakening region operation is not in the scope of this paper. This is left as a future research study.

Fig. 5 shows the *dq* frame back EMF constants according to the electrical rotor position ($k_d(\theta_{re})$ and $k_q(\theta_{re})$), which are set up in the look-up tables for torque estimation both in simulation and experiment. The actual line-to-line back EMF waveforms are provided in Appendix II.

The feasibility and practical features of the proposed three-phase conduction DTC of a BLDC motor drive scheme have been evaluated using an experimental test-bed, as shown in Fig. 6. The same conditions are used as in simulation.

Implementations of steady state and transient torque, torque error, q- and d-axis rotor reference frame stator currents, and line-to-line current responses of the proposed DTC of a BLDC motor drive scheme are demonstrated in Fig. 7(a) and (b), respectively, under a 0.5 N·m load torque condition.

The torque reference is changed abruptly from 0.52 to 0.65 N·m at 0.65 s. It is seen in Fig. 7(a) (top) that fast torque response is obtained and the estimated torque tracks the reference torque closely. The reference torque value in the experimental test is selected a little bit higher than the load torque to compensate the friction of the total experimental system such that the rotor speed is kept at steady-state level (30 mechanical rad/s). The torque error between reference and estimated electromechanical torque is shown in the bottom part of Fig. 7(a). The high frequency ripples observed in the torque and current can be minimized by properly selecting the dc-link voltage and torque hysteresis band size.

q- and d-axis currents used in (11) are illustrated in Fig. 7 (b), respectively, under 0.5 N·m load torque. At 0.65 seconds the torque reference is increased and the change in the q-axis frame current is noted in Fig. 7(b) (top). In the same figure, the q-axis current fluctuates around a dc offset to obtain smooth electromagnetic torque. It is seen in Fig. 7(b) (top) that the d-axis current oscillates around the desired zero reference value, which means that the stator flux amplitude equals the magnet flux.

The $\alpha\beta$-axes stator flux linkages are estimated using (12) in which the $\alpha\beta$-axes voltages are measured using a dc-link voltage sensor and the estimated position of the stator flux linkage vector θ_s. The motor is initially locked at zero position (phase a) for proper starting. Fig. 8 shows the experimental results of the

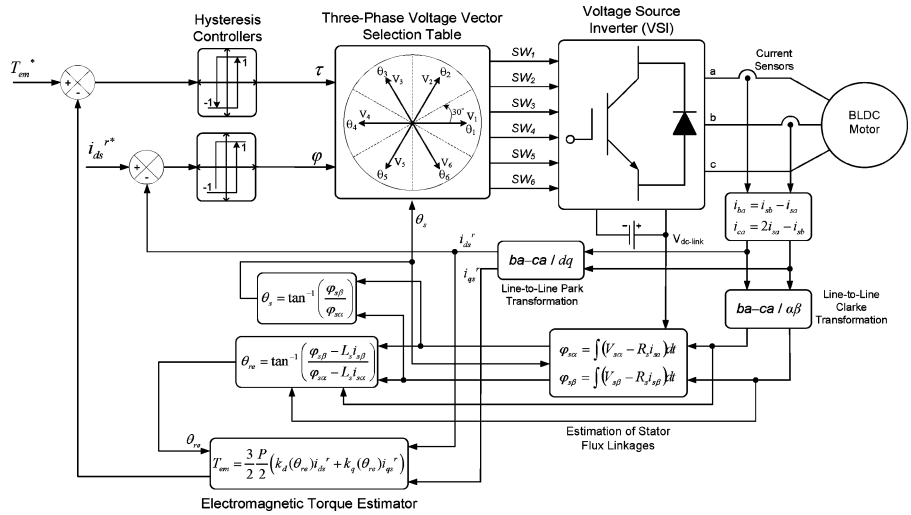

Fig. 3. Overall block diagram of the position-sensorless direct torque and indirect flux control (DTIFC) of BLDC motor drive using three-phase conduction mode.

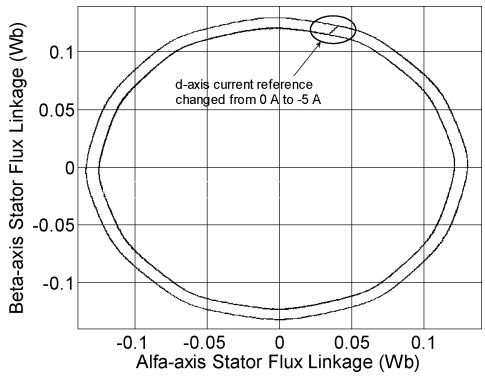

Fig. 4. Simulated indirectly controlled stator flux linkage trajectory under the sensorless three-phase conduction DTC of a BLDC motor drive when i_{ds}^{r*} is changed from 0 to -5 A under 0.5 N·m load torque.

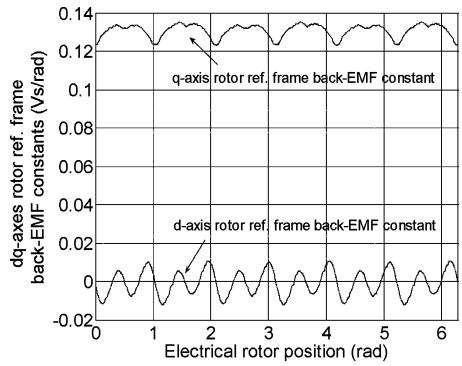

Fig. 5. Actual q- and d-axis rotor reference frame back EMF constants versus electrical rotor position ($k_d(\theta_{re})$ and $k_q(\theta_{re})$).

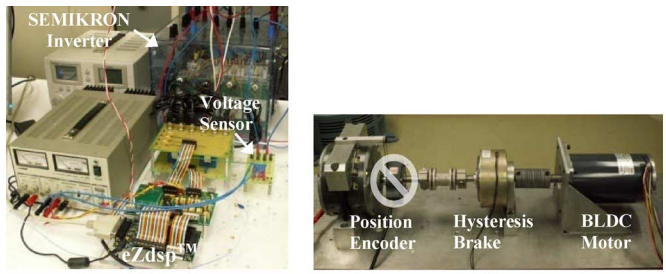

Fig. 6. Experimental test-bed. (a) Inverter and DSP control unit. (b) BLDC motor ($T_{\mathrm{em\_rated}} = 1.28352$ N·m) coupled to dynamometer and position encoder (2048 pulse/revolution) is not used in the control system.

indirectly controlled stator flux linkage locus by controlling the d-axis rotor reference frame current at 0 A when 0.5 N·m load torque is applied to the BLDC motor. The dodecagon shape in the stator flux locus is observed in Fig. 8 due to the nonsinusoidal waveform of the actual back EMFs. Because the actual line-to-line back EMF is not completely uniform over one electrical cycle, peak value of the stator flux linkage along the trajectory ($\alpha\beta$ frame) may vary slightly. It is seen in Fig. 8 that the amplitude of the stator flux linkage, which is the amplitude of the magnet flux linkage, is indirectly controlled quite well at its required value in the constant torque region.

Actual and estimated electrical rotor positions are shown in Fig. 9(a) (top to bottom), respectively. The experimental estimated electrical rotor position is capable of tracking the actual position quite well. In Fig. 9(b), the error between actual and estimated electrical rotor position is illustrated. Close to every maximum position a spike is seen. This is because of the slight phase error between the actual and estimated position. Overall, the error is quite minimal. The electrical rotor position error and electromechanical torque for a long run of 20 s are shown in Fig. 10, respectively. It can be seen that the proposed method is able to drive the BLDC motor without any stability or drift problem. Spikes in the position error data are removed; therefore, the average position error can be seen clearly in Fig. 10 (top). The quality of torque control is evaluated with the time-varying reference, as shown in Fig. 11 where trapezoidal waveform is applied as a reference torque. It can be seen in Fig. 11 that the estimated torque tracks the reference quite well.

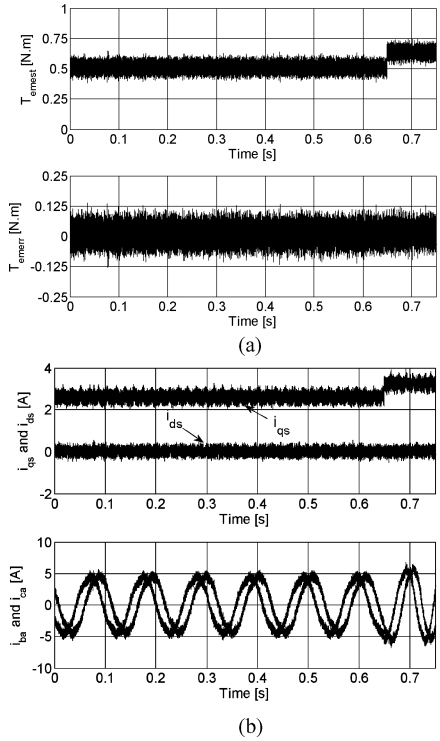

Fig. 7. Steady state and transient behavior of the experimental. (a) (Top) estimated electromagnetic torque, (bottom) error between reference and estimated electromagnetic torque. (b) (Top) q-axis stator current and d-axis stator current and (bottom) *ba–ca* frame currents when $i_{ds}^{r*} = 0$ under 0.5 N·m load torque.

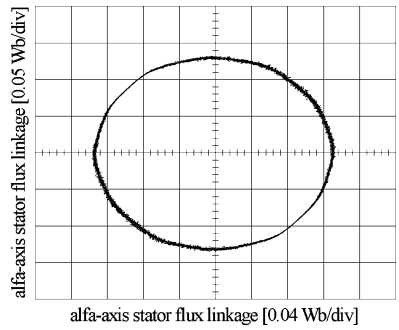

Fig. 8. Experimental indirectly controlled stator flux linkage trajectory under the sensorless three-phase conduction DTC of a BLDC motor drive when $i_{ds}^{r*} = 0$ at 0.5 N·m load torque.

In Fig. 12, the flux-weakening operation is evaluated under 1.1926 N·m load torque. Fig. 12(a) shows the high speed operation when $i_{ds}^{r*} = 0$. The desired speed is dropped from 540 electrical rad/s to 513.5 electrical rad/s and oscillations in speed and torque are observed, as shown in Fig. 12(a). This result shows that the desired torque can only be obtained at lower speed when flux is not weakened. However, in Fig. 12(b), i_{ds}^{r*} is decreased to -4.51 A and the speed is controlled in the desired level quite well. The dc-link voltage is 115 V and the base speed for that voltage is 500 electrical rad/s. Moreover, the space vector PWM technique can be applied to the proposed DTC scheme to minimize the high frequency current and torque ripples as in [33]. Because the estimation algorithm depends on the winding inductance as well as resistance, their variations

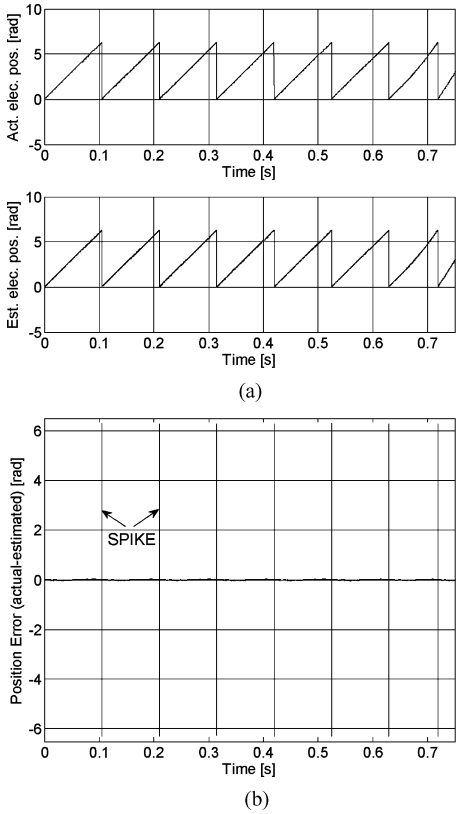

Fig. 9. (a) Steady state and transient behavior of the actual and estimated electrical rotor positions from top to bottom, respectively and (b) error between actual and estimated electrical rotor positions under 0.5 N·m load torque.

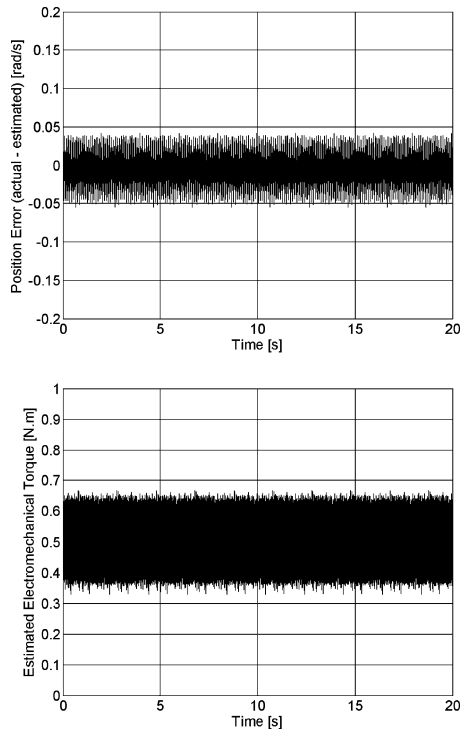

Fig. 10. (Top) Steady-state behavior of the experimental electrical rotor position error and (bottom) estimated electromechanical torque when $i_{ds}^{r*} = 0$ under 0.5 N·m load torque.

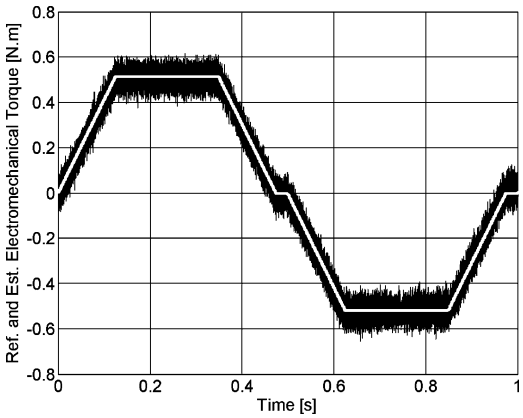

Fig. 11. Experimental estimated electromechanical torque under time-varying reference when $i_{ds}^{r*} = 0$ under 0.5 N·m load torque.

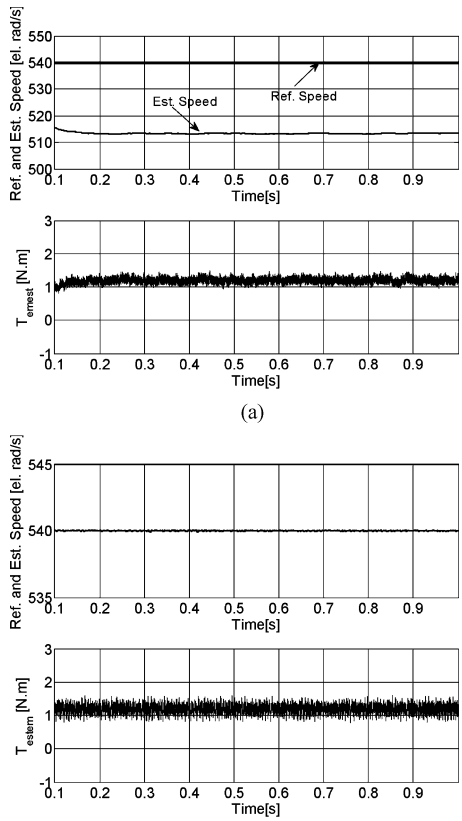

Fig. 12. Steady-state flux-weakening behavior of the experimental actual speed and estimated electromechanical torque, respectively, (a) when $i_{ds}^{r*} = 0$ and (b) when $i_{ds}^{r*} = -4.51$ A under 1.1926 N·m load torque at 540 electrical rad/s desired speed ($V_{\mathrm{dc\_link}} = 115$ V).

should also be considered. However, these are left as future research studies.

V. Conclusion

This paper has successfully demonstrated application of the proposed position-sensorless three-phase conduction DTC scheme for BLDC motor drives that is similar to the conventional DTC used for sinusoidal ac motors where both torque and flux are controlled, simultaneously. This method provides advantages of the classical DTC such as fast torque response compared to vector control, simplicity (no PWM strategies, PI controllers, and inverse Park and inverse Clarke transformations), and a position-sensorless drive. It is shown that the BLDC motor could also operate in the flux-weakening region by properly selecting the d-axis current reference in the proposed DTC scheme. First, practically available actual two line-to-line back EMF constants (k_{ba} and k_{ca}) versus electrical rotor position are obtained using generator test and converted to the *dq* frame equivalents using the new line-to-line Park transformation in which only two input variables are required. Then, they are used in the torque estimation algorithm. Electrical rotor position required in the torque estimation is obtained using winding inductance, stationary reference frame currents, and stator flux linkages.

Since the actual back EMF waveforms are used in the torque estimation, low-frequency torque oscillations can be reduced convincingly compared to the one with the ideal-trapezoidal waveforms having 120 electrical degree flat top. A look-up table for the three-phase voltage vector selection is designed similar to a DTC of PMSM drive to provide fast torque and flux control. Because the actual rotor flux linkage is not sinusoidal, stator flux control with constant reference is not viable anymore. Therefore, indirect stator flux control is performed by controlling the flux related d-axis current using bang-bang (hysteresis) control, which provides acceptable control of time-varying signals (reference and/or feedback) quite well.

Appendix I

Specifications and Parameters of the BLDC Motor

Symbol	Quantity	Value
P	Number of poles	4
V_{LL}	Maximum line-to-line voltage (V_{rms})	115
I_{pk}	Maximum peak current (A)	24
I_{rated}	Rated current (A)	5.6
T_{rated}	Rated torque (N·m)	1.28352
L_s	Winding inductance (mH)	1.4
M	Mutual inductance (mH)	0.3125
R_s	Winding resistance (ohm)	0.315
λ_f	Rotor magnetic flux linkage (Wb)	0.1146

Appendix II

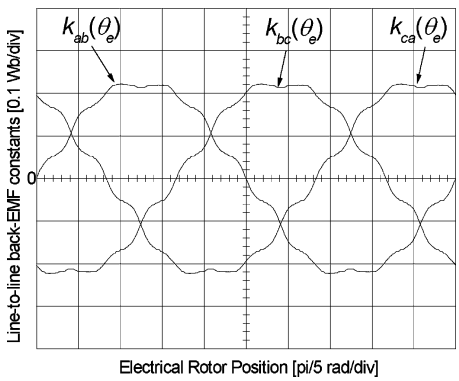

ACKNOWLEDGMENT

The first author (S. B. Ozturk) would like to thank A. Toliyat of the University of Texas at Austin for his assistance in editing the paper.

REFERENCES

[1] W. C. Gan and L. Qiu, "Torque and velocity ripple elimination of AC permanent magnet motor control systems using the internal model principle," *IEEE/ASME Trans. Mechatronics*, vol. 9, no. 2, pp. 436–447, Jun. 2004.

[2] D. Sun and J. K. Mills, "Torque and current control of high-speed motion control systems with sinusoidal-PMAC motors," *IEEE/ASME Trans. Mechatronics*, vol. 7, no. 3, pp. 369–377, Sep. 2002.

[3] H. Melkote and J. Khorrami, "Nonlinear adaptive control of direct-drive brushless DC motors and applications to robotic manipulators," *IEEE/ASME Trans. Mechatronics*, vol. 4, no. 1, pp. 71–81, Mar. 1999.

[4] H. R. Bolton and R. A. Ashen, "Influence of motor design and feed current waveform on torque ripple in brushless dc drives," *Proc. Inst. Elect. Eng.—Elect. Power Appl.*, vol. 131, no. 3, pp. 82–90, 1984.

[5] B. H. Ng, M. F. Rahman, and T. S. Low, "An investigation into the effects of machine parameters on torque pulsation in a brushless dc drive," in *Proc. IEEE IECON*, 1988, pp. 749–754.

[6] H. Le-Huy, R. Perret, and R. Feuillet, "Minimization of torque ripple in brushless dc motor drives," *IEEE Trans. Ind. Appl.*, vol. IA-22, no. 4, pp. 748–755, Jul./Aug. 1986.

[7] F. Piriou, A. Razek, R. Perret, and H. Le-Huy, "Torque characteristics of brushless dc motors with imposed current waveform," in *Conf. Rec. IEEE IAS Annu. Meeting*, 1986, pp. 176–181.

[8] D. Hanselman, "Minimum torque ripple, maximum efficiency excitation of brushless permanent magnet motors," *IEEE Trans. Ind. Electron.*, vol. 41, no. 3, pp. 292–300, Jun. 1994.

[9] N. Matsui, T. Makino, and H. Satoh, "Auto-compensation of torque ripple of DD motor by torque observer," *IEEE Trans. Ind. Appl.*, vol. 29, no. 1, pp. 187–194, Jan./Feb. 1993.

[10] T. S. Low, K. J. Tseng, T. H. Lee, K. W. Lim, and K. S. Lock, "Strategy for the instantaneous torque control of permanent-magnet brushless dc drives," *Proc. Inst. Elect. Eng.—Elect. Power Appl.*, vol. 137, no. 6, pp. 355–363, Nov. 1990.

[11] T. S. Low, T. H. Lee, K. J. Tseng, and K. S. Lock, "Servo performance of a BLDC drive with instantaneous torque control," *IEEE Trans. Ind. Appl.*, vol. 28, no. 2, pp. 455–462, Mar./Apr. 1992.

[12] K. Y. Cho, J. D. Bae, S. K. Chung, and M. J. Youn, "Torque harmonics minimization in permanent magnet synchronous motor with back-EMF estimation," in *Proc. IEE Elec. Power Appl.*, vol. 141, no. 6, pp. 323–330, 1994.

[13] D. Grenier, L. A. Dessaint, O. Akhrif, and J. P. Louis, "A park-like transformation for the study and the control of a nonsinusoidal brushless dc motor," in *Proc. IEEE IECON*, Orlando, FL, Nov. 6–10, 1995, vol. 2, pp. 836–843.

[14] F. Bodin and S. Siala, "New reference frame for brushless dc motor drive," in *Proc. IEE-PEVD Annu. Meeting*, London, U.K., Sep. 21–23, 1998, pp. 554–559.

[15] D. Grenier, S. Yala, O. Akhrif, and L. A. Dessaint, "Direct torque control of pm ac motor with non-sinusoidal flux distribution using state-feedback linearization techniques," in *Proc. IEEE IECON*, Aachen, Germany, Aug. 31–Sep. 4, 1998, vol. 3, pp. 1515–1520.

[16] T. Kim, H.-W. Lee, L. Parsa, and M. Ehsani, "Optimal power and torque control of a brushless dc (BLDC) motor/generator drive in electric and hybrid electric vehicles," in *Conf. Rec. IEEE IAS Annu. Meeting*, 8–12 Oct. 2006, vol. 3, pp. 1276–1281.

[17] I. J. Ha and C. I. Kang, "Explicit characterization of all feedback linearizing controllers for a general type of brushless dc motor," *IEEE Trans. Autom. Control*, vol. 39, no. 3, pp. 673–677, Mar. 1994.

[18] F. Aghili, M. Buehler, and J. M. Hollerbach, "Experimental characterization and quadratic programming-based control of brushless motors," *IEEE Trans. Control Syst. Technol.*, vol. 11, no. 1, pp. 139–146, Jan. 2003.

[19] S. J. Kang and S. K. Sul, "Direct torque control of brushless dc motor with nonideal trapezoidal back-EMF," *IEEE Trans. Power Electron.*, vol. 10, no. 6, pp. 796–802, Nov. 1995.

[20] S. K. Chung, H. S. Kim, C. G. Kim, and M. J. Youn, "A new instantaneous torque control of PM synchronous motor for high-performance direct-drive applications," *IEEE Trans. Power Electron.*, vol. 13, no. 3, pp. 388–400, May 1998.

[21] P. J. Sung, W. P. Han, L. H. Man, and F. Harashima, "A new approach for minimum-torque-ripple maximum-efficiency control of BLDC motor," *IEEE Trans. Ind. Electron.*, vol. 47, no. 1, pp. 109–114, Feb. 2000.

[22] L. Hao and H. A. Toliyat, "BLDC motor full-speed operation using hybrid sliding mode observer," in *Proc. IEEE APEC*, Miami, FL, Feb. 9–13, 2003, vol. 1, pp. 286–293.

[23] P. L. Chapman, S. D. Sudhoff, and C. A. Whitcomb, "Multiple reference frame analysis of non-sinusoidal brushless dc drives," *IEEE Trans. Energy Convers.*, vol. 14, no. 3, pp. 440–446, Sep. 1999.

[24] I. Takahashi and T. Noguchi, "A new quick-response and high-efficiency control strategies of an induction motor," *IEEE Trans. Ind. Appl.*, vol. 22, no. 5, pp. 820–827, Sep./Oct. 1986.

[25] M. Depenbrock, "Direct self-control of inverter-fed induction machine," *IEEE Trans. Power Electron.*, vol. 3, no. 4, pp. 420–429, Oct. 1988.

[26] L. Zhong, M. F. Rahman, W. Y. Hu, and K. W. Lim, "Analysis of direct torque control in permanent magnet synchronous motor drives," *IEEE Trans. Power Electron.*, vol. 12, no. 3, pp. 528–536, May 1997.

[27] Y. Liu, Z. Q. Zhu, and D. Howe, "Direct torque control of brushless dc drives with reduced torque ripple," *IEEE Trans. Ind. Appl.*, vol. 41, no. 2, pp. 599–608, Mar./Apr. 2005.

[28] S. B. Ozturk and H. A. Toliyat, "Direct torque control of brushless dc motor with non-sinusoidal back-EMF," in *Proc. IEEE IEMDC Biennial Meeting*, Antalya, Turkey, May 3–5, 2007, vol. 1, pp. 165–171.

[29] P. J. Sung, W. P. Han, L. H. Man, and F. Harashima, "A new approach for minimum-torque-ripple maximum-efficiency control of BLDC motor," *IEEE Trans. Ind. Electron.*, vol. 47, no. 1, pp. 109–114, Feb. 2000.

[30] L. Zhong, M. F. Rahman, W. Y. Hu, and K. W. Lim, "Analysis of direct torque control in permanent magnet synchronous motor drives," *IEEE Trans. Power Electron.*, vol. 12, no. 3, pp. 528–536, May 1997.

[31] S. B. Ozturk and H. A. Toliyat, "Sensorless direct torque and indirect flux control of brushless dc motor with non-sinusoidal back-EMF," in *Proc. IEEE IECON*, Orlando, FL, Nov. 9–11, 2008, pp. 1373–1378.

[32] J. Hu and B. Wu, "New integration algorithms for estimating motor flux over a wide speed range," *IEEE Trans. Power Electrons.*, vol. 13, no. 5, pp. 969–977, Sep. 1998.

[33] K. Gulez, A. A. Adam, and H. Pastaci, "A novel direct torque control algorithm for IPMSM with minimum harmonics and torque ripples," *IEEE/ASME Trans. Mechatronics*, vol. 12, no. 2, pp. 223–227, Apr. 2007.

Salih Baris Ozturk (S'02–M'08) received the B.S. degree (with honors) from Istanbul Technical University, Istanbul, Turkey, in 2000, and the M.S. and Ph.D. degrees from Texas A&M University, College Station, in 2005 and 2008, respectively, all in electrical engineering.

In 2004, he was with the Whirlpool R&D Center, Benton Harbor, MI. In 2008, he joined the Power Electronics Group, United Technologies Research Center, East Hartford, CT, as a Senior Research Engineer. Since 2009, he has been an Assistant Professor in the Department of Electrical and Electronics Engineering, Okan University, Tuzla/Istanbul, Turkey. His current research interests include power electronics, fault diagnosis of electric machines, and digital-signal-processor-based advanced control of ac drives, in particular, sensorless and direct torque control of permanent-magnet-assisted synchronous reluctance, permanent-magnet synchronous, and brushless dc motors. He is the coauthor of the book *DSP-Based Electromagnetic Motion Control* (Boca Raton, FL: CRC Press, 2003).

Dr. Ozturk received the 2008 IEEE Industrial Electronics Society Second Best Paper Award from the Electric Machines Technical Committee for his paper "Sensorless Direct Torque and Indirect Flux Control of Brushless DC Motor with Non-sinusoidal Back-EMF" presented at the 2008 IEEE Industrial Electronics Conference, Miami, FL. He is also one of the recipients of the 2008 Outstanding Achievement Award (highest award) from the United Technologies Research Center for his participation in achieving the successful demonstration of the World's First Fuel Cell Powered Rotorcraft Flight.

Hamid A. Toliyat (S'87–M'91–SM'96–F'08) received the B.S. degree from Sharif University of Technology, Tehran, Iran, in 1982, the M.S. degree from West Virginia University, Morgantown, in 1986, and the Ph.D. degree from the University of Wisconsin, Madison, in 1991, all in electrical engineering.

After completing the Ph.D. degree, he joined Ferdowsi University of Mashhad, Mashhad, Iran, as an Assistant Professor of electrical engineering. In March 1994, he joined the Department of Electrical and Computer Engineering, Texas A&M University, College Station, where he is currently the Raytheon Endowed Professor of Electrical Engineering. His research interests and experience include analysis and design of electrical machines, variable-speed drives for traction and propulsion applications, fault diagnosis of electric machinery, and sensorless variable-speed drives. He has supervised more than 35 graduate students, published more than 335 technical papers in which more than 100 papers are in IEEE TRANSACTIONS, presented more than 50 invited lectures all over the world, and has ten issued and pending U.S. patents. He is the author of the book *DSP-Based Electromechanical Motion Control* (CRC Press, 2003), and the Co-Editor of *Handbook of Electric Motors—2nd Edition* (Marcel Dekker, 2004).

Dr. Toliyat is a Fellow of the IEEE Power Engineering, IEEE Industry Applications, IEEE Industrial Electronics, and IEEE Power Electronics Societies and a member of Sigma Xi. He is a Professional Engineer in the State of Texas. He received the prestigious Cyrill Veinott Award in electromechanical energy conversion from the IEEE Power Engineering Society in 2004, the Patent and Innovation Award from the Texas A&M University System Office of Technology Commercializations in 2007, the TEES Faculty Fellow Award in 2006, the Distinguished Teaching Award in 2003, the E. D. Brockett Professorship Award in 2002, the Eugene Webb Faculty Fellow Award in 2000, and the Texas A&M Select Young Investigator Award in 1999 from Texas A&M University, the Space Act Award from NASA in 1999, Schlumberger Foundation Technical Awards in 2000 and 2001, the 2008 IEEE Industrial Electronics Society Electric Machines Committee Second Best Paper Award, the 1996 and 2006 IEEE Power Engineering Society Prize Paper Awards and the 2006 IEEE Industry Applications Society Transactions Third Prize Paper Award. He is an Editor of IEEE TRANSACTIONS ON ENERGY CONVERSION, and was an Associate Editor of IEEE TRANSACTIONS ON POWER ELECTRONICS. He is also the Chair of the Industrial Power Conversion Systems Department of the IEEE Industry Applications Society. He was the General Chair of the 2005 IEEE International Electric Machines and Drives Conference held in San Antonio, TX.